AIChE

A General Compartment-Based Population Balance Model for Particle Coating and Layered Granulation

Jianfeng Li
School of Chemical Engineering, Purdue University, West Lafayette, IN 47907

Ben Freireich
School of Mechanical Engineering, Purdue University, West Lafayette, IN 47907

Carl Wassgren
School of Mechanical Engineering, Purdue University, West Lafayette, IN 47907

Dept. of Industrial Physical Pharmacy, Purdue University, West Lafayette, IN 47907

James D. Litster
School of Chemical Engineering, Purdue University, West Lafayette, IN 47907

Dept. of Industrial Physical Pharmacy, Purdue University, West Lafayette, IN 47907

DOI 10.1002/aic.12678
Published online June 14, 2011 in Wiley Online Library (wileyonlinelibrary.com).

In this work, a general multidimensional population balance (PB) model is developed to predict the coating volume distribution on polydisperse particles as a function of time during particle coating in a paddle mixer. The model adopts a compartmental approach to account for coating variation caused by particle flow heterogeneity. Simulations show that for a realistic range of seed particle size polydispersity and coating mass applied, the coating volume distribution depends on the growth rate exponent and seed particle size distribute on, with the coating volume coefficient of variance (CoV) approaching an asymptotic value as the coating-to-particle volume ratio increases. These effects cannot be predicted by simpler one-dimensional models. However, the full two-dimensional PB and simpler one-dimensional models such as Mann's equation do predict similar sensitivity of coating volume CoV to the variation in the compartment model parameters, i.e., to changes in the particle mixing behavior in the vessel. © 2011 American Institute of Chemical Engineers *AIChE J,* 58: 1397–1408, 2012
Keywords: population balance, coating volume coefficient of variance, compartment model, growth rate

Introduction

Over the last several decades, particle coating and layered granulation processes have been widely applied in the manufacture of various products, including pharmaceuticals, food, fertilizers and detergents. In general, a coating suspension is atomized and sprayed onto a bed of mechanically or pneumatically fluidized particles. Particle growth then occurs by either interparticle agglomeration or surface layering. The purpose of the coating unit operation ranges from drug release control, particle surface modification and taste masking, to active component addition. In all these applications,

Correspondence concerning this article should be addressed to J. D. Litster at jlitster@ purdue.edu.

one general measure of final product quality is the coating uniformity, which describes the variability of the amount of coating material distributed between each individual particle.

Only a few studies have investigated the coating uniformity over polydisperse particles. One early model[1] assumes that the coating material is evenly distributed when the seed particles have a narrow size distribution. However, experimental results obtained from a fluidized bed coating process show that layering growth is not uniform for all particles.[2] In addition, real particles typically have a nonuniform size distribution. Some experimental observations[3,4] support a linear coating growth assumption, which states that the coating thickness is independent of particle size and thus the coating volume per particle is proportional to its surface area. Subsequent studies have shown a dependence of coating thickness on particle size for some systems.[5–8] In these latter studies, it is reported that the amount of coating volume received is approximately proportional to particle volume rather than particle surface area. These studies reason that the overall growth rate deviates from the surface area. Proportional law is either due to particles' preferential visit to the spray region, or because of the shielding effects in the spray region. Whereas, an opposite trend has been observed that preferential coating occurs on smaller particles in certain spray system.[9] To date, there has been no consensus on the particle size dependency because a mechanistic understanding on the role of particle size on the growth kinetics is missing.

The particle flow patterns in mixing and coating equipment also have a profound influence on coating distributions.[10,11] As coating typically occurs in a small region near a bed's free surface, only a small fraction of particles are exposed to the liquid suspension. To obtain a narrow coating distribution, the occurrence and duration of particles passing through this spray region should be well controlled because the total coating received by an individual particle is the accumulation of many short time sprays as the particle passes through the spray region.[12,13] The mixing efficiency is mainly affected by the operating conditions, such as the mixing rate, the spray rate, and the fill level. Previous studies have shown that a large mixing rate, small spray rate, and small fill level of particles result in a better coating uniformity.[14,15]

Turton[16] recently reviewed various modeling approaches for predicting film coating uniformity. These models are classified into particle level and process level approaches, depending on the scale of scrutiny. The population balance (PB) method is one of the process level modeling tools used to track the evolution of particle property distributions. The application of compartment-based PB modeling to coating processes can be traced back to the 1980s.[1,14,17] To account for the fact that particles are not all sprayed simultaneously, the entire coating vessel is conceptually decomposed into several perfectly mixed regions, with particles circulating between these compartments at a defined rate. Key model variables include the relative size of the spray compartment, the flow rate between compartments, the spray rate, and the spray time.

In recent years, this approach has been widely applied to predict the coating performance in various coaters. For example, Maronga and Wnukowski[18] applied a three domain compartment model to a fluidized bed coater. The three domains consisted of a spray region, a drying region, and a dead zone. The authors found that an increase in the size of the dead zone results in a broader coating distribution, while an increase in the particle circulation rate had the opposite effect. Ronsse et al.[19] and Hede et al.[20] described a fluidized bed coater with a stack of well-mixed compartments in which the coating is assumed to be applied only in the few top compartments. The temperature and moisture difference along the bed height were also monitored simultaneously with a heat and mass balance. Similarly, Denis et al.[21] adopted a twin zone compartment model to investigate the coating process in a rotary drum. Their model consisted of a well-mixed spray region and a plug flow nonspray region. Experiments were also conducted to examine the influence of the process conditions such as fill level and paddle speed. Apart from the work of Freireich et al. (submitted) discussed below, there have been no such studies of compartment-based PB models for coating in mechanical mixers.

The value of a compartment-based PB model as a predictive tool is limited by the ability of the model to accurately account for the effects of operating variables on the particle flow and mixing in the vessel. Few attempts have been made to validate whether or not such models capture the dynamics of particle movement in a coating vessel. Recently, the current authors have developed a multiscale framework to fill this gap. In this new approach, a discrete element method (DEM) simulation is first performed to model the particle mixing in the coating environment. After that, the particle circulation and residence time distributions in the spray zone are collected. This flow information is then captured with a multicompartment model. The modeling approach has been verified for a case study of particle flow in a mechanically agitated mixer by comparing the cumulative residence time distribution in the spray zone from the compartment model with that directly from the DEM simulation,[22] while the DEM simulation results was further validated against an experimentally measured spray zone residence time distribution. The final step is to generate a PB model based on the compartment model structure to simulate the evolution of the coating distribution. This approach combines the particle level (such as DEM) and process level (such as PB) modeling approaches as defined by Turton.[16]

To extend Freireich et al.'s approach to modeling the coating volume distribution over polydisperse particles, it is necessary to develop a two-dimensional (2-D) PB framework. Previously, the particle mass has been chosen to be the single variable tracked in many one-dimensional (1-D) models.[5,8] In these approaches, the coating distribution is obtained by the mass difference in each size interval before and after the simulation. Although this method has also been adopted experimentally in many industrial coating processes, this type of 1-D model does not account for coating variation on particles of similar size because of different exposure times to the coating spray.

The 1-D models with only one particle characteristic property are insufficient to represent the complex physics underlying granulation processes. Several multidimensional PB models have been developed in recent years. Iveson[23] firstly proposed the idea of formulating a three-dimensional PB to track granule size, porosity, and binder content, simultaneously. Poon et al.[24] and Ramachandran et al.[25] have

constructed a multidimensional PB framework to account for the effects of key granule properties on granulation rate processes, including nucleation, aggregation, consolidation, and breakage. Braumann et al.[26] developed a five-dimensional models to incorporate more granulation mechanisms, such as binder solidification and infiltration.

The objective of this work is to predict the coating volume distribution for polydisperse particles based on a multicompartment model. A compartment-based PB model is developed to obtain the 2-D distribution with seed particle volume and coating volume. The model is designed generally to cover a range of mixing models including short circuits and recycle streams. The Freireich et al. (submitted) case study of a Forberg mixer is used to evaluate the effect of particle size distribution on coating quality parameters, and to perform a sensitivity analysis on the parameters of the particle mixing model. The results are compared with predictions from a simpler 1-D coating model.

Model Overview

In the following sections, the development of a general compartment-based PB model to obtain the 2-D distribution with seed particle volume and coating volume is described. The model is then applied to a particular case study of a mixer with nonuniform particle mixing.

Development of a compartment-based PB model

The change in particle properties during the coating process are described with the evolution of a multidimensional distribution $n(\mathbf{X}, \mathbf{R}, t)$, where n is the distribution function indicating the number density of particles which have the internal property state $\mathbf{X}$ and external coordinate state $\mathbf{R}$ at time t. The general PB equation is represented as follows,[27]

$$\frac{\partial n}{\partial t}+\frac{\partial}{\partial \mathbf{X}}\cdot(\mathbf{G_x}n)+\frac{\partial}{\partial \mathbf{R}}\cdot(\mathbf{G_R}n)=\Re_{\text{birth}}-\Re_{\text{death}}, \quad (1)$$

where $\mathbf{G_x}$ and $\mathbf{G_R}$ corresponds to the rates of change of the properties $\mathbf{X}$ and positions $\mathbf{R}$. The terms containing $\mathbf{G_x}$ and $\mathbf{G_R}$ account for the growth and spatial flow mechanisms, respectively. The terms $\Re_{\text{birth}}$ and $\Re_{\text{death}}$ represent the rates of change in the distribution due to discontinuous birth and death events, such as nucleation, agglomeration, and breakage. These mechanisms are often negligible in many coating applications containing large, strong particles [5,18,21], i.e., $\Re_{\text{birth}}=\Re_{\text{death}}=0$.

For dilute particulate flows carried by a continuous fluid phase, the PB can be directly coupled to the flow field through coupled CFD-PB methods. Several CFD-PB coupling methods also adopt the multicompartmental approach by laying one PB equation on each grid cell generated in the CFD simulation.[28] As a similar simulation tool, DEM is well established for dense particulate system such as the ones of interest here. To fully track the particle trajectories and properties from DEM with Eq. 1 is very computational intensive, especially for dense flow particulate systems. Instead, the compartmental approach can be used to provide similar flow field heterogeneity with a network of well-mixed compartments (Figure 1). Thus, the complexity of the PB model is reduced by avoiding tracking of individual particle spatial coordinates while retaining essential

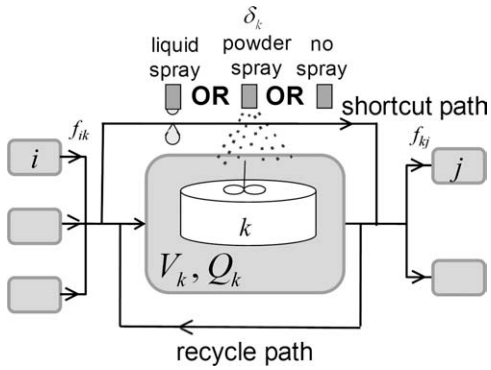

Figure 1. A schematic showing the general attributes of the *k*th compartment.

elements of the heterogeneity of the flow field (Freireich et al., submitted). Each compartment is assigned with a specific spray characteristics, which identifies whether particles inside are sprayed by liquid, powder additives or nothing. The combination of an arbitrary number of compartments, with short circuiting and/or recycle allowed for each compartment gives a flexible scheme to match the complex flow patterns found in different types of equipment.

Equation 1 can be written in row vector form corresponding to the compartment model structure of a particular vessel,

$$\frac{\partial(\overline{\mathbf{Vn}})}{\partial t}+\frac{\partial}{\partial \mathbf{X}}\cdot(\overline{\mathbf{G_x Vn}})=\overline{\mathbf{Qn}_{\text{in}}}-\overline{\mathbf{Qn}_{\text{out}}}, \quad (2)$$

where $\mathbf{V}$ is the volume of the compartment and $\mathbf{Q}$ is a flow rate. The quantities $\overline{\mathbf{Qn}}_{\text{in}}$ and $\overline{\mathbf{Qn}}_{\text{out}}$ are the distribution changes due to the exchange of particles between compartments. The following convention is defined,

$$\overline{\mathbf{ab}}=(a_1b_1 \quad a_2b_2 \quad \cdots \quad a_nb_n). \quad (3)$$

The convective particle flow through the compartments can be represented using a flow matrix $\underline{\underline{\mathbf{f}}}$, with the numerical element f_{jk} describing the fraction of the flow through compartment k that comes from compartment j.

For each compartment, the particle distribution for the outlet flow is the same composition as that within the compartment (representative overflow), while the distribution for the inlet flow is the combination of the distributions of all the compartments that have particles entering into the compartment,

$$\mathbf{n}_{\text{out}}=\mathbf{n}, \quad (4)$$

$$\mathbf{n}_{\text{in}}=\mathbf{n}_{\text{out}}\cdot\underline{\underline{\mathbf{f}}}. \quad (5)$$

Thus, substituting Eqs. 4 and 5 into Eq. 2 results in,

$$\frac{\partial(\overline{\mathbf{Vn}})}{\partial t}+\frac{\partial}{\partial \mathbf{X}}\cdot(\overline{\mathbf{G_x Vn}})=\overline{\mathbf{Qn}\cdot\left(\underline{\underline{\mathbf{f}}}-\underline{\underline{\mathbf{I}}}\right)}. \quad (6)$$

It is convenient to use de-convoluted particle properties, such as solid volume v_{a} and liquid volume v_{l}, as the internal variables tracked with the PB model. For a nonporous particle system, the 2-D function $n_{\text{k}}(v_{\text{a}}, v_{\text{l}})$ is used to represent the

particle distribution in a specific compartment k. Other properties of interest can be obtained from a coordinate transform, e.g., the particle size x is calculated as follows,

$$x = \sqrt[3]{\frac{1}{\alpha_v}(v_a + v_l)}, \tag{7}$$

where α_v is the shape factor that relates particle volume to its size.

Equation 6 can be explicitly written for the kth compartment as,

$$\frac{\partial(V_k n_k)}{\partial t} + \frac{\partial}{\partial v_a}\cdot\left(G_{v_a,\,k} V_k n_k\right) + \frac{\partial}{\partial v_l}\cdot\left(G_{v_l,\,k} V_k n_k\right) = Q_k \sum_j \left(n_j f_{jk}\right) - Q_k n_k. \tag{8}$$

In addition to the relations for the distributions in each compartment, overall mass balance relations due to liquid and powder spray must hold,

$$\sum_k \left(\int_{v_a} \int_{v_l} G_{v_l,\,k} V_k n_k dv_l dv_a \right) = \eta_l \dot{Y}_l, \tag{9}$$

$$\sum_k \left(\int_{v_a} \int_{v_l} G_{v_a,\,k} V_k n_k dv_l dv_a \right) = \eta_a \dot{Y}_a, \tag{10}$$

where $G_{v_l,k}$ and $G_{v_a,k}$ are the microscale growth rates indicating the liquid and solid volume increase of an individual particle, $\dot{Y}_l$ and $\dot{Y}_a$ are the macroscale liquid and powder spray rates, and η_l and η_a are the corresponding spray efficiencies.

Typically, the growth rates $G_{v_l,k}$ and $G_{v_a,k}$ are proportional to the particle volumes raised to a given power,

$$G_{v_l,\,k} = \left(\frac{dv_l}{dt}\right)_k = \delta_{v_l,\,k}\alpha_{v_l,k}(v_a + v_l)^{r_a}, \tag{11}$$

$$G_{v_a,\,k} = \left(\frac{dv_a}{dt}\right)_k = \delta_{v_a,\,k}\alpha_{v_a,k}(v_a + v_l)^{r_l}, \tag{12}$$

where $\delta_{v_a,k}$ and $\delta_{v_l,k}$ are the Boolean variables indicating the spray type of the compartment k, $\alpha_{v_a,k}$ and $\alpha_{v_l,k}$ are the proportionality constants, and r_a and r_l are the exponents acting on the particle volume. The parameter δ_{v_a} is one for compartments with powder feed and zero for all other compartments. The parameter δ_{v_l} is one for compartments with liquid feed and zero for all other compartments.

The PB model is solved using a finite volume method. The particle property domain (v_a, v_l) is discretized into 2-D cells. The cell average number density for compartment k with the cell center indexed as (p, q), $\bar{n}_{k,p,q}$, is given by,

$$\bar{n}_{k,p,q} = \frac{1}{\Delta v_a \Delta v_l} \int_{v_{l,\,q-\frac{1}{2}}}^{v_{l,\,q+\frac{1}{2}}} \int_{v_{a,\,p-\frac{1}{2}}}^{v_{a,\,p+\frac{1}{2}}} n_k dv_a dv_l \tag{13}$$

where $\Delta v_a = v_{a,\,p+\frac{1}{2}} - v_{a,\,p-\frac{1}{2}}$ and $\Delta v_l = v_{l,\,q+\frac{1}{2}} - v_{l,\,q-\frac{1}{2}}$ are the solid volume and liquid volume interval sizes for each cell.

Table 1. Property Vectors for the Spray and Bed Compartment Example Described in the Text

Parameter	Symbol	Value
Volume	$\mathbf{v}$	$[V_1\ V_2]$
Flow rate	$\mathbf{Q}$	$[Q\ Q]$
Flow composition		
	$\underline{\underline{\mathbf{f}}}$	$\begin{bmatrix} 0 & 1 \\ 1 & 0 \end{bmatrix}$
Number density distribution	$\mathbf{N}$	$[n_1\ n_2]$
Growth rate	$\mathbf{Gx}$	$[G\ 0]$

The following discrete form is obtained by performing the operation $\frac{1}{\Delta v_a \Delta v_l}\int_{v_{l,\,q-\frac{1}{2}}}^{v_{l,\,q+\frac{1}{2}}}\int_{v_{a,\,p-\frac{1}{2}}}^{v_{a,\,p+\frac{1}{2}}}(\cdot)dv_a dv_l$ on both sides of Eq. 8,

$$\frac{d\bar{n}_{k,p,q}}{dt} + \frac{1}{\Delta v_a}\left(G_{v_a,\,k,p+\frac{1}{2},q} n_{k,p+\frac{1}{2},q} - G_{v_a,\,k,p-\frac{1}{2},q} n_{k,p-\frac{1}{2},q}\right) + \frac{1}{\Delta v_l}\left(G_{v_l,\,k,p,q+\frac{1}{2}} n_{k,p,q+\frac{1}{2}} - G_{v_l,\,k,p,q-\frac{1}{2}} n_{k,p,q-\frac{1}{2}}\right) = \frac{Q_k}{V_k}\cdot\left(\sum_{j\neq k}\left(\bar{n}_{j,p,q}\cdot f_{jk}\right) - \bar{n}_{k,p,q}\right), \tag{14}$$

and the discrete forms for the growth rate (Eqs. 11 and 12) after substituting for α_k from Eqs. 9 and 10 are,

$$G_{v_l,\,k,s,p} = \frac{\delta_{v_l,\,k}\left(v_{a,p} + v_{l,q}\right)^{r_a}}{\sum_k \delta_{v_l,\,k} V_k \sum_p \sum_q \left(v_{a,p} + v_{l,q}\right)^{r_a} \bar{n}_{k,s,p} \Delta v_a \Delta v_l}\eta_l \dot{Y}_l, \tag{15}$$

$$G_{v_a,\,k,s,p} = \frac{\delta_{v_l,\,k}\left(v_{a,p} + v_{l,q}\right)^{r_l}}{\sum_k \delta_{v_a,\,k} V_k \sum_p \sum_q \left(v_{a,p} + v_{l,q}\right)^{r_l} \bar{n}_{k,s,p} \Delta v_a \Delta v_l}\eta_a \dot{Y}_a. \tag{16}$$

In Eq. 14, the growth fluxes at the cell edges are substituted by the interpolation of the cell averages. For example,

$$G_{v_a,\,k,p+\frac{1}{2},q} n_{k,p+\frac{1}{2},q} = \frac{1}{2}\left(G_{v_a,\,k,p,q}\bar{n}_{k,p,q} + G_{v_a,\,k,p+1,q}\bar{n}_{k,p+1,q}\right). \tag{17}$$

The ordinary differential equation Eq. 14 is solved with a forward Euler time stepping scheme.

As an example, consider the simplest form of a compartment model consisting of two well-mixed compartments with no short circuiting or recycle and liquid spray into the first compartment only. The values of the key flow property variables for this case are shown in Table 1.

Substituting the variables from Table 1 into Eq. 8 results in a set of two PB equations,

$$\frac{\partial(V_1 n_1)}{\partial t} + \frac{\partial(G\cdot V_1 n_1)}{\partial v_l} = Q n_2 - Q n_1, \tag{18}$$

$$\frac{\partial(V_2 n_2)}{\partial t} = Q n_1 - Q n_2. \tag{19}$$

Note that the solid volume growth term in Eq. 8 disappears with the assumption of no powder addition in this case. This two-compartment model is essentially the same as that used by

Figure 2. The Bella XN series dual axis counter rotating paddle mixer modeled in the current study.

Wnukowski and Setterwall[14] to model spray coating in a fluidized bed.

Model application: a case study for particle coating in a Forberg mixer

To demonstrate the predictive ability of this approach, simulations are performed for a batch coating process in a dual-axis paddle mixer (see Figure 2). Details of the mixer configuration and process operation can be found in a previous article (Freireich et al., submitted).

The mechanical mixing of particles was modeled using DEM simulations, and the flow scale information derived from the simulations was represented by residence time distributions for different regions of the mixer (Figure 3). A multicompartment model which reproduces the residence time distributions is given in Figure 4. Details concerning the DEM simulations and compartment model development can also be found in Freireich et al. (submitted).

In this scheme, there is one spray compartment and N-series bed compartments, with extra shortcut and back-mixing paths (Figure 4). The parameter Q is the bulk volumetric flow rate between the spray region and bed region; λ_S and λ_B are the number fractions of particles flowing through the shortcut path in the spray region and bed region, respectively; T_S and T_B are the characteristic time for the single spray compartment and N-series bed compartment, respectively; R is the ratio of the recycle stream to the outflow stream of the bed region.

With the introduction of the short cut and recycle paths, this scheme is capable of simulating the nonideal mixing conditions observed via DEM simulations and experimental studies. The model is robust in that process conditions, such as the fill level and paddle speed, primarily affect the model parameters rather than the model structure itself. The DEM simulations were validated against experimental measurements of spray zone residence time while the compartment model was verified by comparing the residence times against DEM results.[22] The values of the key flow property matrices for the above compartment model are given in Table 2.

The general multidimensional PB model discussed in Section 2.1 is applied using the model parameters listed in Table 2. The two-dimensions v_a and v_l are considered to be the seed particle volume and sprayed liquid volume, respectively. As there is no powder feed in this case, all the terms associated with particle solid volume growth are disappeared. Furthermore, instead of using compartment volume and volumetric flow rate, the mean residence time of the spray zone T_S and that of the bed zone T_B are used with,

$$T_S = \frac{V_S}{(1-\lambda_S)Q}, \tag{20}$$

$$T_B = \frac{V_B}{(1-\lambda_B)(1+R)Q}. \tag{21}$$

The final expressions for the compartment-based PB equations can be written as,

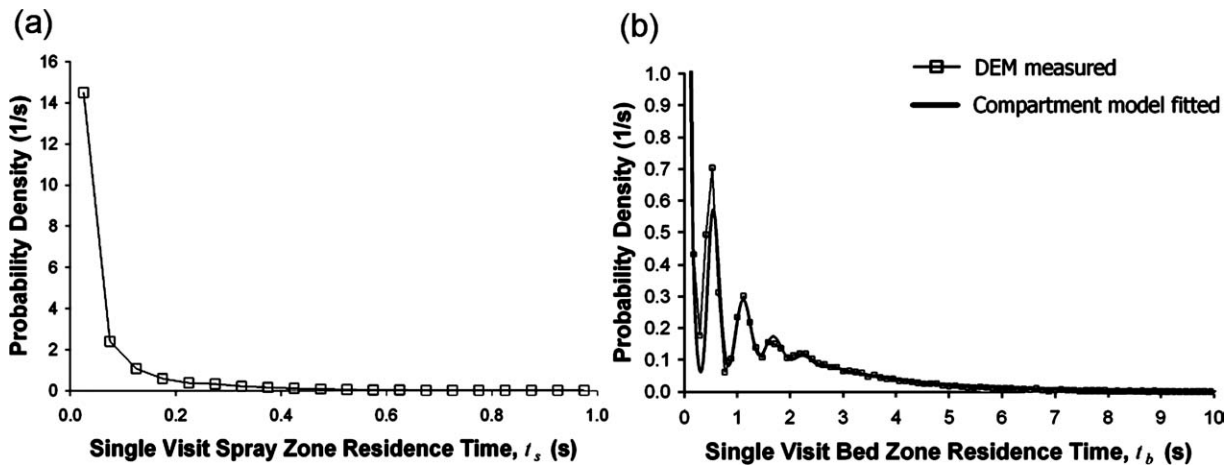

Figure 3. Single visit residence time distributions from the DEM simulations.

(a) For the spray region and (b) for the bed region (Freireich et al., submitted).

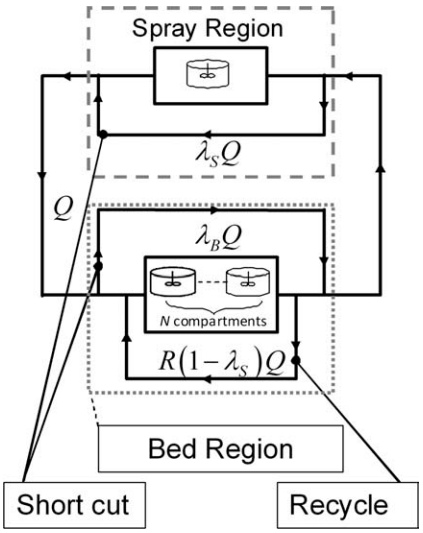

Figure 4. Schematic of the multicompartment model (Freireich et al., submitted).

(a) for the spray zone compartment,

$$\frac{\partial n_S}{\partial t}+\frac{\partial(G\cdot n_S)}{\partial v_S}=\frac{(1-\lambda_S)\lambda_B}{1-\lambda_S\lambda_B}\frac{1}{T_S}n_S+\frac{1-\lambda_B}{1-\lambda_S\lambda_B}\frac{1}{T_S}n_{BN}-\frac{1}{T_S}n_S, \tag{22}$$

(b) for the 1st bed compartment,

$$\begin{aligned}\frac{\partial n_{B1}}{\partial t}&=\frac{1-\lambda_S}{(1-\lambda_S\lambda_B)(1+R)}\cdot\frac{N}{T_B}n_S\\&\quad+\frac{R(1-\lambda_S\lambda_B)+\lambda_S(1-\lambda_B)}{(1-\lambda_S\lambda_B)(1+R)}\cdot\frac{N}{T_B}n_{BN}-\frac{N}{T_B}n_{B1},\end{aligned} \tag{23}$$

(c) for the remainder of the N-1 bed compartments,

$$\frac{\partial n_{Bi}}{\partial t}=\frac{N}{T_B}n_{Bi-1}-\frac{N}{T_B}n_{Bi},\quad i=2\text{ to }N. \tag{24}$$

As liquid feed only exists in the spray zone, the growth rate expression and associated mass balance (Eqs. 9 and 11) reduce to (use r to represent r_l),

$$\int_{v_a}\int_{v_l}GV_S n_S dv_l dv_a=\eta_l\dot{Y}_l, \tag{25}$$

$$G=\alpha_{v_l}(v_a+v_l)^r. \tag{26}$$

The overall distribution n_T is the volumetric average of all the distributions for different compartments,

$$n_T=\frac{\mathbf{V}\cdot\mathbf{n}}{V_T}. \tag{27}$$

Equations 21–27 are discretized using the scheme presented in Section 2.1. The equation set is then solved using a Matlab™ forward Euler routine with an initial time step of $\Delta t = 0.01$ s. During the simulation, the time step Δt is checked and adjusted when necessary to meet the Courant–Friedrichs–Levy (CFL) stability condition, i.e., the time step is restricted so that particles can only grow up to the adjacent size grid within two consecutive time steps. The solid volume and liquid volume interval sizes are chosen to be 0.05 and 0.005 cm^3. For a 100 × 50 grid size system, it takes about 1.5 h computation time to solve for a 300 s simulation time on a desktop computer configured with an Intel Pentium IV 2.2GHz CPU and 2GB RAM. When simulations were run using smaller time steps and liquid and solid volume intervals, there was no difference in the resulting 2-D distributions of liquid and solid volume, confirming that numerical diffusion was not affecting the results.

Table 2. Property Vectors of the Multicompartment Paddle Mixer Model

Parameter	Symbol	Value
Volume	$\mathbf{v}$	$\begin{bmatrix} V_S & \underbrace{\frac{V_B}{N}\ \cdots\ \frac{V_B}{N}}_{N} \end{bmatrix}$
Flow rate	$\mathbf{Q}$	$[(1-\lambda_s)Q\ (1-\lambda_B)(1+R)Q\cdots(1-\lambda_B)(1+R)Q]$
Flow composition	$\underline{\underline{\mathbf{f}}}$	$\begin{bmatrix} \frac{\lambda_B(1-\lambda_S)}{1-\lambda_S\lambda_B} & \frac{(1-\lambda_S)}{(1-\lambda_S\lambda_B)(1+R)} & 0 & \cdots & 0 \\ 0 & 0 & 1 & & 0 \\ \vdots & \vdots & 0 & \ddots & \\ 0 & 0 & \vdots & & 1 \\ \frac{1-\lambda_B}{1-\lambda_S\lambda_B} & \frac{R(1-\lambda_S\lambda_B)+\lambda_S(1-\lambda_B)}{(1-\lambda_S\lambda_B)(1+R)} & 0 & \cdots & 0 \end{bmatrix}$
Number density distribution	$\mathbf{n}$	$[n_S\ n_{B1}\ n_{B2}\cdots n_{BN}]$
Growth rate	$\mathbf{G_x}$	$[G\ 0\cdots 0]$

Results and Discussion

The values of the model parameters applied in the baseline case simulation are given in Table 3. The DEM simulations use identical particle sizes to obtain flow rates between the compartments, which are assumed to be size independent. The compartment model parameters are those fitted to the residence time data from the baseline condition of the DEM simulation (Freireich et al., submitted). In the PB simulation, the breadth of the initial particle size distribution varies over a range that is typical for applications in the literature for coating fertilizers, agricultural seeds, and tablets. The spray rates, spray times, and coating-to-particle volume ratio, are also chosen to be physically realistic for a coating operation of this scale.

Two sets of simulations were performed. First, using the standard compartment mixing model, the particle size distribution, growth law exponent, and spray time were varied to examine the effects of these parameters on the coating distribution, particularly the coating volume CoV which is defined to be the ratio of the variance to the mean of the coating volume distribution. Secondly, a sensitivity analysis was performed on the effects of the compartment model parameters while keeping the initial particle size distribution and spray conditions unchanged.

Table 3. List of Model Parameters for the Baseline Case

Parameter	Value
DEM simulation parameters	
Particle diameter (cm)	1
Number of particles	6000
Impeller speed (RPM)	158
Mixer size (liter)	6
Fitted compartment model parameters with 95% confidence interval	
N	48 ± 11
R	6.453 ± 0.125
T_S (s)	0.118 ± 0.004
T_B (s)	0.630 ± 0.010
λ_S	0.378 ± 0.025
λ_B	0.217 ± 0.003
Q (cm^3/s)	5172.5
PB simulation parameters	
Spray rate, Y_l(ml/min)	150
Spray time (s)	300
Spray efficiency, η	1
Seed particle volume distribution	Lognormal distributed with $CoV_0 = 1$

The effect of growth kinetics

A 2-D particle distribution with respect to seed particle volume v_a and coating volume v_l is obtained in each simulation using Eqs. 22–24. Simulations were performed with log-normal seed size distributions with coefficients of variance of the seed volume varying between 0.125 and 1, and with the final coating-to-seed volume ratio $\bar{v}_l/\bar{v}_a$ set to 0.18.

Figure 5 shows the effect of the growth rate exponent r (Eq. 10) on the generated 2-D coated particle distribution with the same seed size distribution. Different growth laws result in differences in the 2-D distributions of the final products. When the volume growth rate is a constant for all particles ($r = 0$), the average coating volume is independent of the seed particle size distribution. However, if the growth rate is proportional to the particle surface area ($r = 2/3$), or proportional to the particle volume ($r = 1$), the distribution shows a strong dependence of the average coating volume on the seed particle size. The literature reports growth rate exponents in a wide range from 0.67 to 1.2.[5–9] There is no universally "correct" value for r as it will be a strong function of particle flow field and equipment geometry. These 2-D distributions in Figure 5 show the importance for a predictive model to incorporate a suitable growth rate expression corresponding to the specific coating system.

A 1-D coating distribution extracted from the 2-D distribution is as follows,

$$n(v_l) = \int n(v_a, v_l) dv_a, \tag{28}$$

The coating distribution CoV is calculated from $n(v_l)$ at different spray times, i.e., different coating-to-particle volume ratios in Figure 6. In all cases, the coating distribution CoV initially decreases with the spray time. For the constant growth rate ($r = 0$) where the coating is only dependent on the cumulative time in the spray zone, the CoV is inversely proportional to the reciprocal of the square root of the spray time. This result is identical to that expected for a 1-D analysis of the cumulative time in the spray zone (Freireich et al., submitted),and matches the trend expected from the well known analytic expression based on renewal theory.[12,13]

However, the coating distribution CoV evolution deviates from the inverse square root power law behavior for the size dependent growth cases ($r = 2/3$ and $r = 1$). In both cases, the CoV appears to be tending towards asymptotic value as the coating-to-particle volume ratio approaches to 0.1, which is not the case for $r = 0$. This behavior implies much broader coating distributions with a size dependent growth assumption. When the increase in coating variation is caused by particle size differences exceeds that is caused by the differences in the residence time distributions, the CoV will no longer decrease. In general, the limiting value of the CoV increases as the growth exponent r increases.

The effect of the seed particle distribution on the final coating uniformity is also investigated. The coating distributions at the endpoint ($\bar{v}_l/\bar{v}_a = 0.18$), with different seed particle distributions and growth rate exponents, are compared in the form of CoVs (Figure 7). In the constant growth case ($r = 0$), the coating volume CoV is independent of seed size distribution because the coating material is assumed to be distributed evenly among all particles regardless of the particle size. In the other two cases ($r = 2/3$ and $r = 1$) there is a positive correlation between the coating volume CoV and the seed volume CoV_0, with the CoV_0 having a stronger influence as r increases. This result indicates that the seed size distribution influences the extent of the segregation of the coating distribution.

It is worth reflecting on the practical significance of these results. Figures 5 and 6 show that for $r = 2/3$ and $r = 1$, neglecting particle size distribution effects will result in a dramatic underestimate of the coating volume CoV.

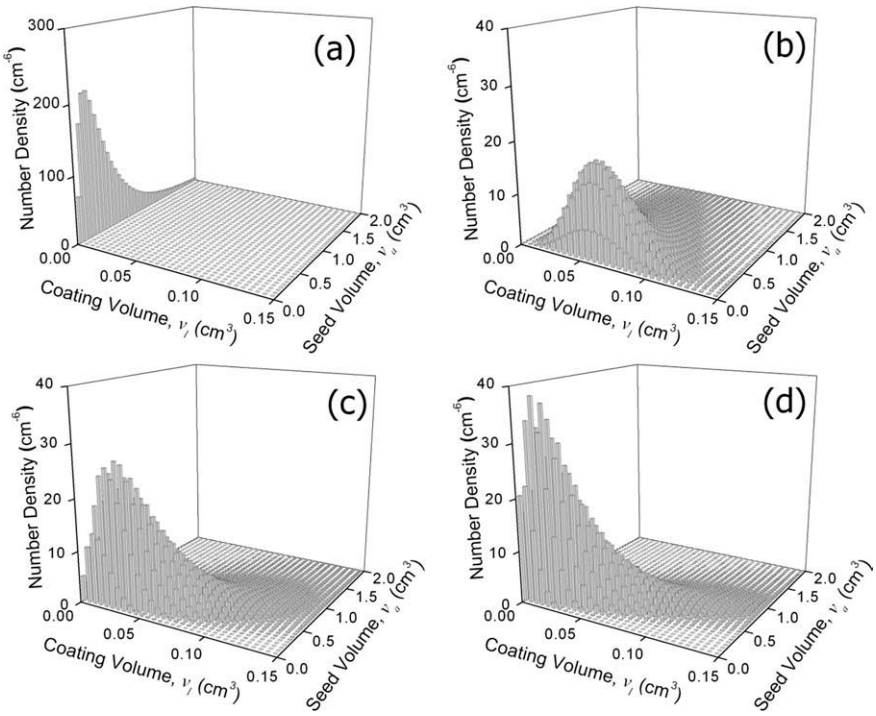

Figure 5. The evolution of 2D particle distribution with various growth kinetics.

(a) Lognormal seed size distribution, (b) $r = 0$, (c) $r = 2/3$, and (d) $r = 1$. In all cases, the seed particle volume $CoV_0 = 1$ and the final coating-to-particle volume is $\bar{v}_l/\bar{v}_a = 0.18$.

Experimental data shows that the growth law exponent falls in this range for most reported systems.[5–8] The figures also show that the error will be minimized if the seed particle volume distribution is very narrow and the coating volume is small compared to the seed particle volume, e.g., coating large pharmaceutical tablets with a thin film. However, many practical systems do not meet these criteria. For example, Braumann et al.[26] showed data for coating feedstock granules where the seed particle volume CoV_0 was ~1.3 and $\bar{v}_l/\bar{v}_a$ was 0.2. Liu and Litster[5] examined fertilizer coatings on agricultural seeds where the CoV_0 varied between 0.1 and 0.3, depending on the seed type and the $\bar{v}_l/\bar{v}_a$ was in the range 0.27–1. For these cases, using a simpler 1-D model, such as Mann's equation (refer to Section 3.2) could lead to both quantitative and qualitative errors in predicting the coating performance.

Sensitivity analysis of compartment model parameters

Previous parametric studies of DEM simulations have demonstrated the flexibility of the compartmental

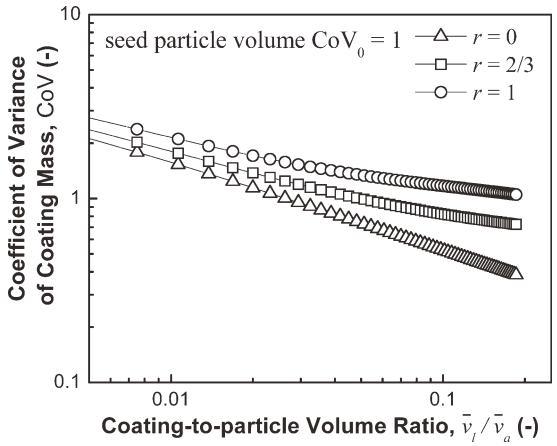

Figure 6. The effect of growth rate exponent *r* on the final coating volume CoV as a function of the spray ratio (compartment model parameters as given in Table 3).

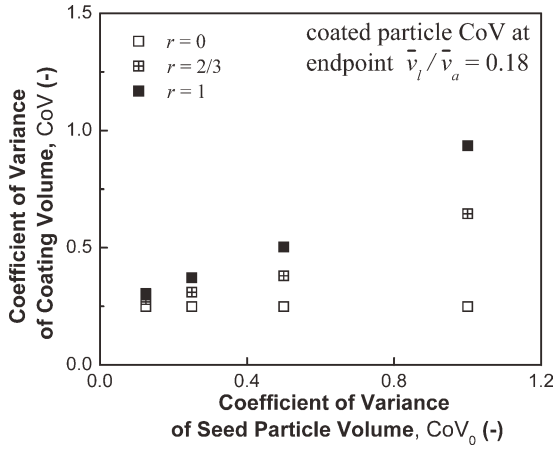

Figure 7. The influence of seed particle volume distribution on the coated particle CoV.

Table 4. The Influence of the Compartment Model Parameters on the Coating Volume Distribution at the Endpoint of $\bar{v}_l/\bar{v}_a = 0.18$

	$\theta_{CoV} = \frac{CoV(X')-CoV(X)}{CoV(X)}$, with model parameter X chosen to be					
$\theta_X = \frac{X'-X}{X}$	N	R	T_S	T_B	λ_S	λ_B
−0.2	0.0005	−0.0573	0.0051	−0.0811	−0.0471	0.0288
−0.1	0.0003	−0.0381	0.0025	−0.0395	−0.0250	0.0146
0.1	−0.0001	0.0272	−0.0025	0.0376	0.0288	−0.0150
0.2	−0.0003	0.0534	−0.0049	0.0734	0.0623	−0.0304

approach.[7,22] Changing the operating parameters such as particle size, paddle speed, and fill ratio mainly affects the value of the compartment model parameters, while the general model structure remains valid. The following section investigates the effects of these model parameters on the coating distribution, with the goal of determining what mixer parameters will lead to optimal coating quality.

The compartment model structure shown in Figure 4 is characterized by six model parameters as defined in Section 2.2: N, R, T_S, T_B, λ_S, and λ_B, which are also the key inputs to the PB model (Eqs. 22–24). A series of simulations were performed by varying one model parameter at a time while keeping the other five parameters constant. While in reality, these parameters are probably varied simultaneously with different mixing condition, they are assumed to be uncoupled from each other in the current study. The baseline parameter set is the same as listed in Table 3, while the relative change in each parameter, θ_X, ranges from −0.2 to +0.2. The results are compared in the form of θ_{CoV}, i.e., the relative change of the coating volume CoV at the endpoint of $\bar{v}_l/\bar{v}_a = 0.18$. In these simulations the growth rate exponent r is chosen to be 2/3. The results of the studies are summarized in Table 4.

The sensitivity of the coating distribution varies depending upon the model parameter. The number of bed compartments N and the mean time through the spray zone T_S have the least influence on the coating distribution. The former is not surprising because the residence time distribution for an N-series tank model approaches plug flow for large N, which is the case in this example. The low sensitivity of the coating distribution to T_S is not intuitive; however, it can be explained as a combination of two effects. First, the value of T_S is relatively small compared to T_B, as the mean spray time only accounts for 2% of the mean circulation time. Thus, the 20% variation in T_S does not invoke much change in the other flow properties, such as the frequency of the spray zone visits. Second, the spray zone is modeled as a well-mixed region with a short cut path. The coating variation arising from the spray duration of a single pass through the spray zone is independent of T_S, as the mean and variance of the residence time are both proportional to T_S.

The recycle ratio R, the mean time across the cascade of tanks T_B, and the spray zone shortcut fraction λ_S all have positive correlation with the coating distribution. An increase in any of these three parameters leads to a larger variation in the time required to make a single pass through the bed zone, which accounts for most of the circulation time. Therefore, the variation in the number of spray zone visits increases, which leads to a broad coating distribution. Finally, a negative dependence of CoV is observed for the bed zone shortcut fraction λ_B, which is in agreement with the opposite trend observed for λ_S. All of these dependences suggest that an increase in the number of spray zone visits can improve the uniformity of the coating distribution.

We can compare these compartment model parametric studies with those obtained from a simpler 1-D CoV equation. With the assumption that the coating volume CoV is proportional to the CoV of the particle cumulative spray visit time (i.e., analogous to $r = 0$), Mann[12] suggested the following equation to calculate the CoV for a general two-compartment system consisting of a spray and bed region,

$$\mathrm{CoV} = \sqrt{\frac{\mu_C}{t}\left[\left(\frac{\sigma_S}{\mu_S}\right)^2 + \left(\frac{\sigma_C}{\mu_C}\right)^2\right]}, \tag{29}$$

where μ_C and σ_C are the mean and standard deviation of circulation time, and μ_S and σ_S are the mean and standard deviation of the single visit spray zone residence time. These statistical values can be substituted (see Appendix) to obtain a CoV expression with the six model parameters listed in Table 4. A sensitivity analysis can then be performed by calculating the partial derivatives of the CoV with each model parameter.

Figure 8 shows that the percentage changes of the coating volume CoV evaluated by the 1-D Mann's equation matches well with those presented in Table 4, even though Mann's equation implicitly assumes size

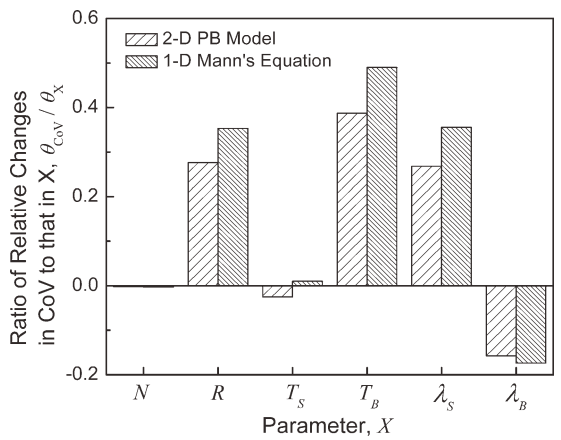

Figure 8. Comparison of the model parameter effects evaluated from the two modeling approaches.

independent growth ($r = 0$). This result implies that the influences of the flow heterogeneity and the particle size distribution on the coating uniformity can be treated separately, at least for this case study. That is to say, if only the operation conditions are changed in the coating process, the percentage change of the coating uniformity can be evaluated from the 1-D CoV equation using the new model parameter values. However, the full 2-D PB model needs to be performed if the seed particle distribution is also changed.

Conclusions

A general two-dimensional PB model was developed to predict the evolution of particle mass and coating mass distribution for particle coating in mechanically or pneumatically agitated coaters and granulators. By using a compartment model structure of the mixer developed from DEM simulations, the model was applied to predict coating uniformity under heterogeneous particle flow conditions in a paddle mixer.

For a physically realistic range of seed particle size polydispersity and coating mass applied, the quality of the coating distribution, as measured by its coefficient of variance, is a strong function of the seed particle size distribution and the growth law expression. Coating mass CoV increases linearly with the seed particle distribution CoV, while the proportionality constant increasing with the growth rate exponent, r. The effect of growth order and seed particle size dispersity on coating mass CoV increases with increasing coating-to-particle volume ratio. As coating-to-particle volume ratio increases, the coating mass CoV approaches an asymptotic minimum value, which is a function of both the growth rate exponent and the initial seed polydispersity. These effects cannot be predicted by simpler one-dimensional models for coating quality.

The CoV of the coating volume is also sensitive to the compartment model parameters, which indicates that the particle flow characteristics in the mixer influence the coating evolution. In general, an increase in the frequency of particles being sprayed improves the coating uniformity. Simplified models such as 1-D Mann's equation are successful in predicting the sensitivity of the coating variability to changes in particle mixing in the coater, even though these 1-D models cannot quantitatively predict the coating variation for a polydisperse system. Thus, the effect of the flow pattern nonuniformities in the mixer on coating performance can be decoupled from the effects of seed particle polydispersity for coating.

Although this article focuses on one particular mechanical mixer design, the structure of the proposed compartment model and associated PB is sufficiently general to address coating and layered granulation for a variety of equipment types, provided that particle mixing data is available from DEM or other sources to fit the compartment model parameters.

Acknowledgment

The authors thank "Procter and Gamble" for their generous support for this work.

Literature Cited

1. Smith PG, Nienow AW. Particle growth mechanisms in fluidized-bed granulation. 2. Comparison of experimental-data with growth-models. *Chem Eng Sci*. 1983;38:1233–1240.
2. Kucharski J, Kmiec A. Kinetics of granulation process during coating of tablets in a spouted bed. *Chem Eng Sci*. 1989;44: 1627–1636.
3. Ragnarsson G, Johansson MO. Coated drug cores in multiple unit preparations influence of particle-size. *Drug Dev Ind Pharm*. 1988;14:2285–2297.
4. Abe E, Yamada N, Hirosue H, Nakamura H. Coating mass distributions of seed particles in a tumbling fluidized bed coater. *Powder Technol*. 1998;97:85–90.
5. Liu LX, Litster JD. Coating mass-distribution from a spouted bed seed coater—experimental and modeling studies. *Powder Technol*. 1993;74:259–270.
6. Sudsakorn K, Turton R. Nonuniformity of particle coating on a size distribution of particles in a fluidized bed coater. *Powder Technol*. 2000;110:37–43.
7. Duarte CR, Murata VV, Barrozo AS. The use of a population balance model in the study of inoculation of soybean seeds in a spouted bed. *Can J Chem Eng*. 2004;82:116–121.
8. Paulo Filho M, Rocha SCS, Lisboa ACL. Modeling and experimental analysis of polydispersed particles coating in spouted bed. *Chem Eng Process*. 2006;45:965–972.
9. Maronga SJ, Wnukowski P. Growth kinetics in particle coating by top-spray fluidized bed systems. *Adv Powder Technol*. 2001;12: 371–391.
10. Choi MMS, Meisen A. Sulfur coating of urea in shallow spouted beds. *Chem Eng Sci*. 1997;52:1073–1086.
11. Becher RD, Schlunder EU. Fluidized bed granulation—the importance of a drying zone for the particle growth mechanism. *Chem Eng Process*. 1998;37:1–6.
12. Mann U. Analysis of spouted-bed coating and granulation. 1. Batch operation. *Ind Eng Chem Process Des Dev*. 1983;22:288–292.
13. Cheng XX, Turton R. The prediction of variability occurring in fluidized bed coating equipment. I. The measurement of particle circulation rates in a bottom-spray fluidized bed coater. *Pharm Dev Technol*. 2000;5:311–322.
14. Wnukowski P, Setterwall F. The coating of particles in a fluidized-bed (residence time distribution in a system of two coupled perfect mixers). *Chem Eng Sci*. 1989;44:493–505.
15. Nakamura H, Abe E, Yamada N. Coating mass distributions of seed particles in a tumbling fluidized bed coater part ii. A Monte Carlo simulation of particle coating. *Powder Technol*. 1998;99:140–146.
16. Turton R. The application of modeling techniques to film-coating processes. *Drug Dev Ind Pharm*. 2010;36:143–151.
17. Sherony DF. A model of surface renewal with application to fluid bed coating of particles. *Chem Eng Sci*. 1981;36:845–848.
18. Maronga SJ, Wnukowski P. Modelling of the three-domain fluidized-bed particulate coating process. *Chem Eng Sci*. 1997;52:2915–2925.
19. Ronsse F, Pieters JG, Dewettinck K. Combined population balance and thermodynamic modelling of the batch top-spray fluidised bed coating process. Part I—model development and validation. *J Food Eng*. 2007;78:296–307.
20. Hede PD, Bach P, Jensen AD. Batch top-spray fluid bed coating: scale-up insight using dynamic heat- and mass-transfer modelling. *Chem Eng Sci*. 2009;64:1293–1317.
21. Denis C, Hemati M, Chulia D, Lanne J-Y, Buisson B, Daste G, Elbaz F. A model of surface renewal with application to the coating of pharmaceutical tablets in rotary drums. *Powder Technol*. 2003; 130:174–180.
22. Freireich B, Li J, Litster JD, Wassgren C. Incorporating particle flow information from discrete element simulations in population balance models of mixer-coaters. *Chem Eng Sci* (2011), DOI, http://dx.doi.org/10.1016/j.ces.2011.04.015.
23. Iveson SM. Limitations of one-dimensional population balance models of wet granulation processes. *Powder Technol*. 2002;124: 219–229.
24. Poon JMH, Immanuel CD, Doyle FJ, Litster JD. A three-dimensional population balance model of granulation with a mechanistic representation of the nucleation and aggregation phenomena. *Chem Eng Sci*. 2008;63:1315–1329.
25. Ramachandran R, Immanuel CD, Stepanek F, Litster JD, Doyle FJ. A mechanistic model for granule breakage in population balances of

granulation: theoretical kernel development and experimental validation. *Chem Eng Res Des*. 2009;87:598–614.
26. Braumann A, Goodson MJ, Kraft M, Mort PR. Modelling and validation of granulation with heterogeneous binder dispersion and chemical reaction. *Chem Eng Sci*. 2007;62:4717–4728.
27. Ramkrishna D. *Population Balances: Theory and Applications to Particulate Systems in Engineering*. San Diego: Academic Press, 2000.
28. Bezzo F, Macchietto S, Pantelides CC. A general methodology for hybrid multizonal/CFD models. Part I. Theoretical framework. *Comput Chem Eng*. 2004;28:501–511.

Appendix: Evaluation of Compartment Model Parameter Effects on Coating CoV with the 1D Mann's Equation

A two-compartment model with spray and bed regions is used to describe the general coating process. With the assumption that the coating volume of an individual particle is proportional to its cumulative residence time in the spray compartment, the coating volume CoV is written as,[12]

$$\mathrm{CoV} = \sqrt{\frac{\mu_C}{t}\left[\left(\frac{\sigma_S}{\mu_S}\right)^2 + \left(\frac{\sigma_C}{\mu_C}\right)^2\right]}, \tag{A1}$$

where μ_C and σ_C are the mean and standard deviation of the circulation time, and μ_S and σ_S are the mean and standard deviation of the single visit spray zone residence time.

Note that particle circulations consist of mutually independent, alternative visits to the spray zone and bed zone,

$$\mu_C = \mu_S + \mu_B, \tag{A2}$$

$$\sigma_C^2 = \sigma_S^2 + \sigma_B^2, \tag{A3}$$

where μ_B and σ_B are the mean and standard deviation of the single visit bed zone residence time.

For the compartment model structure shown in Figure 4, the single visit residence time distribution (SVRTD) for the spray zone is,

$$E_S(t) = \lambda_S\delta(t) + (1-\lambda_S)\frac{1}{T_S}e^{-t\Big/T_S}, \tag{A4}$$

where λ_S is the spray zone shortcut and T_S is the characteristic single visit spray zone time. The SVRTD for the bed zone is,

$$E_B(t) = \lambda_B\delta(t) + (1-\lambda_B)\sum_{n=1}^{\infty}\left[\left(\frac{R}{1+R}\right)^{n-1}\left(\frac{1}{1+R}\right) \times \frac{1}{T_B}\frac{1}{(Nn-1)!}\left(\frac{t}{T_B}\right)^{Nn-1}e^{-\frac{t}{T_B}}\right] \tag{A5}$$

where λ_S is the bed zone shortcut, R is the bed zone recycle amount, T_B is the characteristic single visit bed zone time, and N is the number of bed compartments represents the particle motion characteristics in the bed zone (Freireich et al., submitted).

The means and variances calculated from the distribution $E_S(t)$ and $E_B(t)$ are,

$$\mu_S = (1-\lambda_S)T_S, \tag{A6}$$

$$\sigma_S^2 = (1-\lambda_S^2)T_S^2, \tag{A7}$$

$$\mu_B = (1-\lambda_B)(1+R)T_B, \tag{A8}$$

and,

$$\sigma_B^2 = (1-\lambda_B)(1+R)T_B^2\left[(1+R)\lambda_B + R + \frac{1}{N}\right]. \tag{A9}$$

Substituting Eqs. A2–A9 into Eq. 29, the CoV can be expressed as,

$$\mathrm{CoV} = \sqrt{\frac{(1-\lambda_S)T_S + (1-\lambda_B)(1+R)T_B}{t}\cdot \left\{\frac{1+\lambda_S}{1-\lambda_S} + \frac{(1-\lambda_S^2)T_S^2 + (1-\lambda_B)(1+R)T_B^2\left[(1+R)\lambda_B + R + \frac{1}{N}\right]}{\left[(1-\lambda_S)T_S + (1-\lambda_B)(1+R)T_B\right]^2}\right\}}. \tag{A10}$$

Define the characteristic spray time τ as,

$$\tau = (\mu_S + \mu_B)\left[\left(\frac{\sigma_S}{\mu_S}\right)^2 + \frac{\sigma_S^2 + \sigma_B^2}{(\mu_S+\mu_B)^2}\right], \tag{A11}$$

and the CoV expression of Eq. (A1) simplifies to,

$$\mathrm{CoV} = \sqrt{\frac{\tau}{t}}. \tag{A12}$$

From Eq. A11, τ is a function of the independent model parameters N, R, T_S, T_B, λ_S, and λ_B via the intermediate variables μ_S, μ_B, σ_S^2, and σ_B^2,

$$\tau = f\left[\mu_S(\lambda_S, T_S), \sigma_S^2(\lambda_S, T_S), \mu_B(\lambda_B, R, T_B), \sigma_B^2(\lambda_B, R, T_B, N)\right]. \tag{A13}$$

Sensitivity to the compartment model parameters can be determined by finding the total differential of τ, which can be shown to be,

$$d\tau = \left(\frac{\partial\tau}{\partial\mu_S}\frac{\partial\mu_S}{\partial\lambda_S} + \frac{\partial\tau}{\partial\sigma_S^2}\frac{\partial\sigma_S^2}{\partial\lambda_S}\right)d\lambda_S + \left(\frac{\partial\tau}{\partial\mu_S}\frac{\partial\mu_S}{\partial T_S} + \frac{\partial\tau}{\partial\sigma_S^2}\frac{\partial\sigma_S^2}{\partial T_S}\right)dT_S + \left(\frac{\partial\tau}{\partial\mu_B}\frac{\partial\mu_B}{\partial\lambda_B} + \frac{\partial\tau}{\partial\sigma_B^2}\frac{\partial\sigma_B^2}{\partial\lambda_B}\right)d\lambda_B + \left(\frac{\partial\tau}{\partial\mu_B}\frac{\partial\mu_B}{\partial R} + \frac{\partial\tau}{\partial\sigma_B^2}\frac{\partial\sigma_B^2}{\partial R}\right)dR + \left(\frac{\partial\tau}{\partial\mu_B}\frac{\partial\mu_B}{\partial T_B} + \frac{\partial\tau}{\partial\sigma_B^2}\frac{\partial\sigma_B^2}{\partial T_B}\right)dT_B + \frac{\partial\tau}{\partial\sigma_B^2}\frac{\partial\sigma_B^2}{\partial N}dN \tag{A14}$$

The partial derivatives of the CoV with respect to each model parameter can be evaluated using the chain rule. For example, the partial derivative of the CoV to the shortcut fraction λ_S is,

$$\frac{\partial \mathrm{CoV}}{\partial \lambda_S} = \frac{\mathrm{CoV}}{2\tau} \cdot \frac{\partial \tau}{\partial \lambda_S}. \tag{A15}$$

The ratio of relative percentage change in CoV to that in λ_S is,

$$\frac{\theta_{\mathrm{CoV}}}{\theta_{\lambda_S}} = \frac{\frac{\partial \mathrm{CoV}}{\mathrm{CoV}}}{\frac{\partial \lambda_S}{\lambda_S}} = \frac{\lambda_S}{\mathrm{CoV}} \cdot \frac{\partial \mathrm{CoV}}{\partial \lambda_S}. \tag{A16}$$

From Eqs. A14–A16,

$$\frac{\theta_{\mathrm{CoV}}}{\theta_{\lambda_S}} = \frac{\lambda_S}{2\tau}\left(\frac{\partial \tau}{\partial \mu_S}\frac{\partial \mu_S}{\partial \lambda_S} + \frac{\partial \tau}{\partial \sigma_S^2}\frac{\partial \sigma_S^2}{\partial \lambda_S}\right). \tag{A17}$$

while the partial derivatives in Eq. A17 can be obtained directly from Eqs. A6–A11.

The effects of other model parameters can be evaluated in a similar manner.

Manuscript received Feb. 9, 2011, and revision received May 2, 2011.